Comparative analysis of sensible heat and latent heat packed bed cold energy storage for liquid air energy storage systems

Mashayekh, Afshin; Hwan Park, Jung; Desai, Nishith Babubhai; Lee, Jeong Ik; Haglind, Fredrik

Published in:
Proceedings of ECOS 2023 - The 36th International Conference on Efficiency, Cost, Optimization, Simulation and Environmental Impact of Energy Systems 2023

Link to article, DOI:
10.52202/069564-0203

Publication date:
2023

Document Version
Peer reviewed version

Comparative analysis of sensible heat and latent heat packed bed cold energy storage for liquid air energy storage systems

Afshin Mashayekh[a], Jung Hwan Park[b], Nishith Babubhai Desai[c], Jeong Ik Lee[d], Fredrik Haglind[e]

[a] Technical University of Denmark, Department of Civil and Mechanical Engineering, 2800 Kongens Lyngby, Denmark, afmas@dtu.dk, CA
[b] Korea Advanced Institute of Science and Technology, Department of Nuclear and Quantum Engineering, Daejeon, South Korea, junghwanpark@kaist.ac.kr
[c] Technical University of Denmark, Department of Civil and Mechanical Engineering, 2800 Kongens Lyngby, Denmark, nbdes@dtu.dk
[d] Korea Advanced Institute of Science and Technology, Department of Nuclear and Quantum Engineering, Daejeon, South Korea, jeongiklee@kaist.ac.kr
[e] Technical University of Denmark, Department of Civil and Mechanical Engineering, 2800 Kongens Lyngby, Denmark, fhag@dtu.dk

Abstract:

A liquid air energy storage is a novel technology receiving substantial interest for balancing the supply and demand of energy because of its high energy density and not being geographically constrained. The main challenge of the liquid air energy storage system demonstrated so far is its low round-trip efficiency. Internal heat recovery, using hot and cold thermal energy storages, increases the round-trip efficiency of the liquid air energy storage. High temperature thermal energy storages are widely studied for different applications. However, the poor performance of the cold thermal energy storage is currently a bottleneck to achieve cost-effectiveness of the liquid air energy storage system. That is due to the very low temperatures and the large temperature span of the cold energy storage. In this paper, two types of cold thermal energy storages, a packed-bed sensible storage and a latent heat storage with cryogenic phase change materials, were applied to a stand-alone liquid air energy storage system. A one-dimensional transient numerical model was developed to analyse the storage systems. The round-trip efficiency, liquid air yield, and expansion work of the liquid air energy storage system were evaluated considering both storage options. The results indicate that the latent heat packed bed storage configuration has higher round-trip efficiency (41 %), liquid yield (58.1 %), and power output (42 MW) than those of the configurations with sensible heat storage. However, there are some sensible materials, like quartzite rocks that, with the same volume of the packed bed, perform as well as cryogenic phase change materials due to their high densities.

Keywords:

Cold thermal energy storage; Latent heat storage; Liquid air energy storage; Packed bed rock thermal energy storage; Phase change materials; Sensible heat storage.

1. Introduction

Large-scale energy storage systems are promising options to mitigate the variability of renewable energy sources and to balance the energy supply and demand [1,2]. Liquid air energy storage (LAES) is a novel technology that has recently gained increasing attention. The LAES system is not geographically restricted and requires much less storage volume than those of the more mature technologies – in the order of 700 times less than that of compressed air energy storage [3,4]. The LAES system comprises three processes: 1) charging process – excess electricity (e.g. from wind and/or solar energy) is used to drive a liquefaction process, 2) storing process – liquid air is stored in cryogenic tanks at nearly ambient pressure, and 3) discharging process – the liquid air is pressurized, regasified and expanded in turbines producing electricity. At present, the LAES technology is at an industrial demonstration level. The main challenge that the LAES system confronts is its low round-trip efficiency, the ratio of the electricity generated during the discharging process to the electricity consumed during the charging process, in comparison to other energy storage systems such as a compressed air energy storage [5]. The round-trip efficiency of the LAES system can be improved by introducing hot and cold thermal energy storages, which allow for the internal recuperation of

hot and cold fluid streams. However, the designs of the heat exchangers and thermal energy storages present some challenges – specifically with respect to the cold thermal energy storage system. So far, various studies have been conducted on High-Grade Cold Energy Storage (HGCS). Broadly speaking, HGCS can be divided into three types: storage using fluids (methanol and propane) [6], using packed beds (such as rock and pebbles) [7], and using phase change material (PCM) [8]. So far, various research studies on LAES systems have been done specifically focused on cold storage systems with different designs, and a majority of those consider packed bed rock storage systems.

Wang et al. [9] applied a dynamic model to analyse the performance of a standalone LAES system by using sensible heat packed bed rock storage for both the cold and hot energy storages, achieving a round-trip efficiency of 43 %. She et al. [4] studied an LAES system with a two fluids system for the cold energy storages and thermal oil for hot energy storage and attained a round-trip efficiency of 53 %. Ryu et al. [10] analysed a LAES system based on the Linde-Hampson refrigeration cycle using a combination of sensible and latent heat packed bed storage systems as the cold energy storage unit. A round-trip efficiency of 60.6 % was obtained. In this case the required temperature for liquefying air could be provided continually during the phase change of the PCM. Tafone et al. [11] investigated a cold thermal energy storage for the LAES system by using a cryogenic PCM. It was found that by using cryogenic PCM as the storage medium, the temperature at the outlet of the packed bed is limited by the melting point of PCM and therefore, the temperature of the heat transfer fluid at the inlet of cold box is lower than the case with sensible heat particles which reduces the compressor power requirement.

Bashiri Mousavi et al. [12] studied a packed bed with three layers of different PCM as a cold storage system of the LAES system and reached a round-trip efficiency of 42.5 % when the system has reached equilibrium. They designed the packed bed's tank with the PCM with lowest melting point located at the bottom of the tank and the PCM with highest melting point placed at the top of the tank. Sciacovelli et al. [13] used a modular packed bed system filled with quartzite rocks. They validated their numerical model with experimental of the LAES pilot plant available at the University of Birmingham, UK. They also investigated the effect of charging and discharging pressure on the round-trip efficiency of the LAES system. It was observed that there is an optimum value for charging pressure that results in the maximum round-trip efficiency (50 % under nominal conditions). Guo et al. [14] developed a dynamic model to analyse the packed bed as the cold energy storage in the LAES system. Granite was used as the storage material and the results suggested that because of both the intermittent period between charging and discharging cycles and the cold energy loss, the round-trip efficiency is 16.8% lower than that of the ideal system in quasi-steady state. Tafone et al. [15] developed a performance map for the LAES system. They investigated the effect of various parameters including turbomachinery isentropic efficiency, storage pressure of liquefied air in the tank, efficiency of hot and cold energy storage, charging and discharging pressure, and the ratio of recirculation mass flow rate. It was observed that increasing the liquid air tank pressure enhances the heat capacity of the recirculation fluid. In turn, this increases the efficiency of the cold box unit, and, as a result, the system's performance becomes independent of the charging pressure.

Wang et al. [16] applied a two tanks system with pressurized propane as the heat transfer fluid for cold energy storage in the LAES system and obtained an electrical round-trip efficiency of 50 % as well as a combined heat and electricity efficiency of up to 81%, using the excess heat available in the hot energy storage system as the heat source. Hüttermann and Span [17] studied nine different storage materials in a packed bed for the cold energy storage unit of the LAES system. The results demonstrated that the system with lead has the maximum efficiency of the packed bed cold storage among other materials due to its lower variation of specific heat capacity over the temperature span than that of the other storage particles. Peng et al. [18] developed a model to investigate the performance of an LAES with sensible heat packed bed (using rocks as the particles) as the cold energy storage. They found that the round-trip efficiency of LAES system is affected by the inlet temperature of cold box, charge and discharge pressure. A maximum round-trip efficiency of 62 % is reachable for optimal conditions for the LAES system.

Storage systems with two working fluids have the disadvantage of using working fluids that are usually flammable [9] and the necessity and using four tanks, increasing the complexity for industrial applications.[9] In this context, a packed bed energy storage system with sensible or latent heat particles is a promising technology for cold storage systems for industrial LAES systems. This technology can relatively easy be integrated into the LAES system and covers the entire temperature range of the cold storage in a single tank. In addition, because of large latent heat of PCMs, PCM based storage has a high energy density, which makes it suitable as a storage medium.

The objective of this paper is to identify the optimum storage medium for cold storage packed bed system in stand-alone LAES systems. Three different materials were investigated: quartz and silicon dioxide as sensible materials and an alcohol-based fluid as latent heat PCM. The materials are used in the form of particles placed in a tank. A thermodynamic model of the LAES system integrated with a 1-dimensional transient numerical model of the packed bed system was developed. The round-trip efficiency, liquid yield, and turbine output are compared for the three different cold thermal energy storage units for the LAES system. There is only a single previous study available in the open literature comparing sensible and latent

heat materials for packed bed cold storage for LAES applications [11]. However, in Ref. [11] different storage materials for the packed bed cold storage were evaluated solely in terms of storage performance. In contrast, the current paper presents, for the first time, an analysis of the effects of different storage materials for the packed bed cold storage on the LAES performance. Such analysis will be useful both for industry and academia for the future development of cold energy storage units for LAES systems.

In the following, section 2 discusses the methods. Section 3 presents and discusses the results obtained from numerical simulations, while section 4 summarizes the conclusions of the work.

2. Methods

2.1 System description

Figure 1 shows a schematic diagram of a liquid air energy storage system (LAES) with two tank hot and packed bed cold energy storages. The proposed system consists of a charging cycle and discharging cycle. The charging cycle consists of multi-stage compressors, air-oil heat exchangers with the thermal oil VP1, a cold-box, a cryo-turbine, a gas-liquid separator, and a liquid air tank. The discharging cycle consists of a cryo-pump, an evaporator, air-oil heat exchangers, and multi-stage turbines. In order to utilize the cold energy, a cold packed bed storage is located between the charging and discharging cycles. Packed bed storage improves the cycle efficiency by exchanging heat between the charging and discharging processes. When the electricity price is low, the air is compressed through multi-stage compressors. Initially, the cold packed bed storage transfers cold energy to the compressed air, causing the temperature of point A7 to decrease to a cryogenic temperature (A8) inside the cold box. After the cooling process, compressed air is expanded to ambient pressure through a cryo-turbine and separated into liquid (A_Liq) and gaseous forms (A10). At peak hours (during a discharge process), liquid air is evaporated while the cold energy is stored in the packed bed cold storage. Gaseous air is heated in the thermal oil heat exchangers and expanded through air turbines to generate electricity.

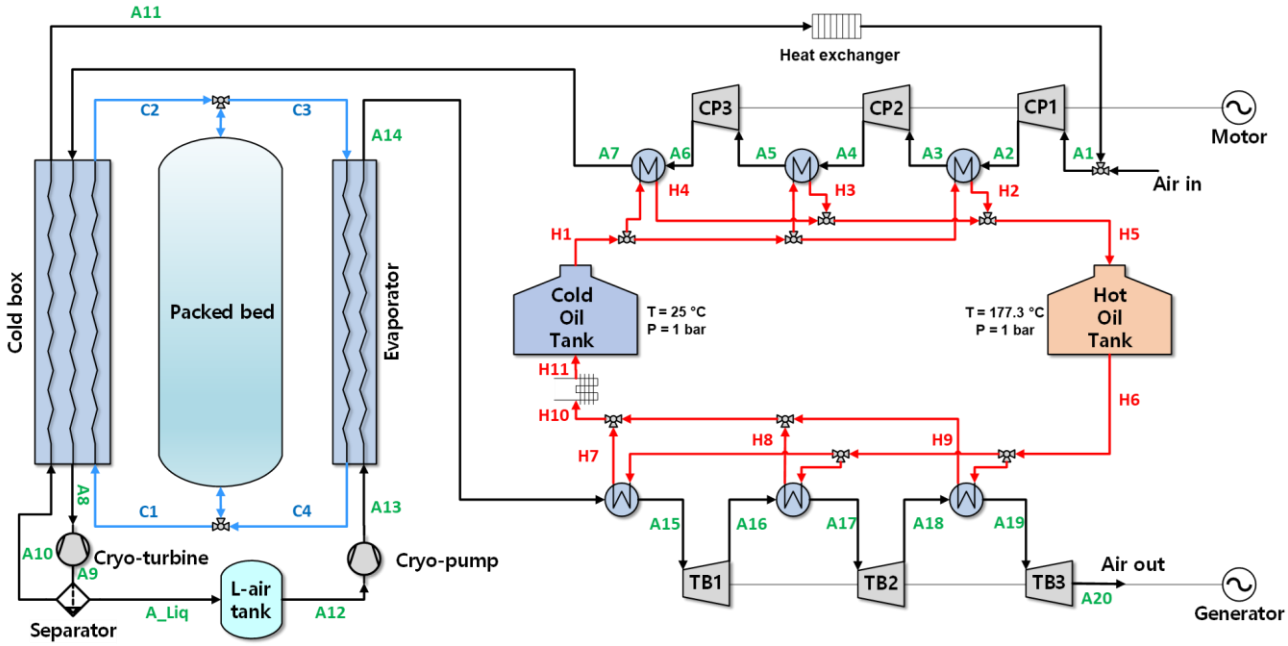

Figure. 1. *Schematic diagram of liquid air energy storage system with cold packed bed storage (CP and TB stand for compressor and turbine, respectively).*

The input parameters of the system are presented in Table 2. The design charging cycle power input (96 MWe), hot thermal energy storage capacity (800 MWh_{th}) and volume (9000 m^3), cold thermal energy storage systems' volume (15000 m^3), and charging time (8 hrs) were fixed for the analysis. The design discharging cycle power output is calculated based on the available liquid yield during charging cycle and discharge duration of 8 hrs. In order to achieve 96 MW of power input for the LAES charging cycle, 17 MPa was selected as the fitting charging pressure. It is worth to note that the LAES system is designed as a large-scale electricity storage system, which require a large volume of the packed bed storage for cold thermal energy as well as a large volume of tanks for the hot thermal energy.

Due to manufacturing constraints of packed bed systems, the diameter of the tank must not exceed 6 m, and the recommended H/D ratio for packed bed systems based on literature is 2 [19,20]. Based on these considerations, the packed bed's height and inner diameter were set to 12 m and 6 m, respectively. In order to achieve the total storage capacity needed for the system, a series of packed beds in a parallel

configuration was used. In total 44 packed bed tanks are needed, which means that the input of the packed bed system (C2 during LAES charging and C4 during LAES discharging) was divided among 44 packed bed tanks. Similarly, the outlet streams of the packed bed tanks were collected, leading to the desired outlet flow of the packed bed system (C1 during LAES charging and C3 during LAES discharging). In order to avoid the use of multiple cold energy storage tanks, it may be a possibility to use one or a few underground packed bed storage tanks [21], however, in this case the LAES system will not be geographically unconstrained, which is one of the major advantages of the LAES technology.

Table. 2. *Input parameters for the system modelling.*

Parameter	$Value$
Particle diameter	0.02 m
Ambient temperature	293 K
Ambient pressure	101 KPa
Charging pressure	17 MPa
Packed bed initial temperature	101.47 K
Pinch points:	
Air-Oil heat exchangers	5 K
Cold box	2 K
Evaporator	2 K
Turbomachinery isentropic efficiency [9]:	
Compressors	89 %
Cryo-turbines	90 %
Cryo-pump	80 %
Gas turbines	75 %

2.2 Component thermodynamic model

In order to simulate the proposed system, the mathematical modelling of the components is implemented into the MATLAB environment. The specific enthalpy change is modelled by the isentropic efficiency model. The compressor power input, $\dot{W}_C$, and the gas turbine power, $\dot{W}_T$, are calculated as follows:

$$\dot{W}_C = \dot{m}(h_{out} - h_{in}) = \dot{m}(h_{out.is} - h_{in})/\eta_{CP} \quad (1)$$

$$\dot{W}_T = \dot{m}(h_{in} - h_{out}) = \eta_{TB} \times \dot{m}(h_{in} - h_{out.is}) \quad (2)$$

where $\dot{m}$ is mass flow rate, h is specific enthalpy, and η is the isentropic efficiency of each component.

Heat exchangers are modelled with basic heat balance equations. The heat exchangers are assumed to be counter-flow heat exchangers and a pinch point limitation is applied.

$$\dot{Q}_{hot} = \dot{m}_{hot}(h_{H_{in}} - h_{H_{out}}) \quad (3)$$

$$h_{C_{out}} = h_{C_{in}} + \frac{\dot{Q}_{hot}}{\dot{m}_{cold}} \quad (4)$$

Pinch point: $min(T_{hot} - T_{cold}) = 5K$ (5)

where $\dot{Q}$ represents the heat transfer rate, h_H and h_C are specific enthalpy of the hot side and cold side, respectively. Subscripts in and out represent the inlet and outlet stream.

The multi-stream cold box is the most important component in the proposed system because the liquid air yield and round-trip efficiency are directly affected by its performance. Compressed air is cooled down to cryogenic temperature by compressed cold air from cold packed bed storage. For simplifying the multi-stream heat exchanger's calculation, it is assumed that there is no heat transfer between cold side fluids. Also, the outlet temperatures of the fluids on the cold side are imposed. The heat transfer rate of the hot side fluid and objective pinch point temperature are calculated as follows:

$$\dot{Q}_{hot} = \dot{m}_{hot}\left(h_{H_{in}} - h_{H_{out}}\right) = \dot{Q}_{pacekd\ bed} + \dot{Q}_{recycle} \quad (6)$$

Pinch point: $min\left(min\left(T_H - T_{packed\ bed}\right), min\left(T_H - T_{recycle\ air}\right)\right) = 5K$ (7)

where $\dot{Q}$ represents heat transfer rate, and T_{fluid} is the temperature of each fluid.

As the modelling is transient, and the mean liquid yield is calculated as follows:

$$Y = \frac{1}{t_{ch}} \int_0^{t_{ch}} y.\, dt \quad (8)$$

The round-trip efficiency is defined as the ratio of the total electricity generation in the discharging process to the power consumption in the charging process:

$$\eta_{RTE} = \frac{W_{discharging}}{W_{charging}} = \frac{\int_0^{t_{dis}} \dot{W}_T - \dot{W}_{CRP} dt}{\int_0^{t_{ch}} \dot{W}_C - \dot{W}_{CTB} dt} \quad (9)$$

where the subscripts CRP and CTB represents the cryo-pump and cryo-turbine, respectively.

2.3 Packed bed modelling

For calculating the heat transfer performance of packed bed storage, the energy balance equation is used. The energy equation for fluid and solid particles presents in Eq. (10) and Eq. (11), respectively. The packed bed storage is considered a 1D cylindrical tank and radial distribution of temperature based on Eq. (12) is considered inside the particles.

The following assumptions were made:

1. The distribution of velocity in the entire packed bed tank is constant and uniform. This assumption is valid for systems with $D/d_p > 30$ [22].
2. The heat transfer mechanism between the heat transfer fluid and particles are convection and conduction. Radiation is neglected.
3. The porosity is uniform along the packed bed tank.
4. The particles are of the same size and spherical shape.
5. The heat loss of the tank to the ambient is considered.

$$\varepsilon \rho_f c_{p.f} \left(\frac{\partial T_f}{\partial t} + u_f \frac{\partial T_f}{\partial z} \right) = \varepsilon k_f \frac{\partial^2 T_f}{\partial z^2} + \frac{6(1-\varepsilon)}{d_p} h_{fp} \left(T_s - T_f \right) + h_w \left(T_w - T_f \right) \quad (10)$$

$$(1-\varepsilon) \rho_s c_{p.s} \frac{\partial T_s}{\partial t} = (1-\varepsilon) k_s \frac{\partial^2 T_s}{\partial z^2} + \frac{6(1-\varepsilon)}{d_p} h_{fp} \left(T_f - T_s \right) \quad (11)$$

$$\rho_p c_{p.p} \frac{\partial T_p}{\partial t} = k_p \left(\frac{\partial^2 T_p}{\partial r^2} + \frac{1}{r} \frac{\partial T_p}{\partial r} \right) \quad (12)$$

where ε is the porosity of the packed bed, ρ is density, c_p is the specific heat of fluid, k is thermal conductivity, d_p is the particle diameter, h_{fp} is the heat transfer coefficient of fluid to solid, h_w is the heat transfer coefficient of heat loss to the ambient, and T is temperature. Subscripts f, p, and s are fluid, particle, and solid, respectively.

In order to model the thermophysical properties of the PCM, an effective heat capacity method is used [23]. The latent heat is represented as a sensible heat spread over a finite temperature difference. Thus, the specific heat of PCM is defined among three phases, namely solid, solid-liquid transition, and liquid phases:

$$c_{p.p} = \begin{cases} c_{p.s} & T_p < T_{m1} \\ \frac{c_{p.s} + c_{p.f}}{2} + \frac{L_H}{Tm2 - Tm1} & T_{m1} < T_p < T_{m2} \\ c_{p.f} & T_p > T_{m2} \end{cases} \quad (13)$$

$$k_{p.p} = \begin{cases} k_{p.s} & T_p < T_{m1} \\ \frac{k_{p.s} + k_{p.f}}{2} & T_{m1} < T_p < T_{m2} \\ k_{p.f} & T_p > T_{m2} \end{cases} \quad (14)$$

where T_{m1} and T_{m2} represent the solidification and melting temperatures of the PCM during the solid-liquid transition, and L_H is the latent heat. For updating the air properties which are temperature dependant, the REFPROP library [24] is used and applied to the model.

In order to solve the energy balance equation, boundary conditions and initial conditions are specified for the fluid and solid:

$$T_f(z=0) = T_{in}; \quad \frac{\partial T_f}{\partial z}(z=H) = 0 \quad (15)$$

$$T_s(z=0) = T_{in}; \frac{\partial T_s}{\partial z}(z=H) = 0 \quad (16)$$

$$T_f(t=0) = T_{in}; T_s(t=0) = T_o \quad (17)$$

$$\frac{\partial T_p}{\partial r}(r=0) = 0; \quad T_p\left(r = \frac{R}{2}\right) = T_s \quad (18)$$

where T_{in} is the packed bed inlet temperature, T_o is the initial temperature, and T_s is the solid temperature. Figure 2 depicts a schematic view of a packed bed filled with particles.

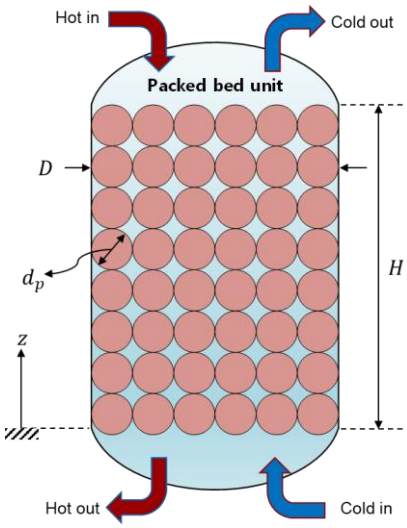

Figure. 2. *Schematic view of 1D packed bed with geometry indicators.*

In order to apply heat transfer between the fluid and solid, an empirical correlation is applied. For the Nusselt number, the following correlation is used [25]:

$$Nu = \frac{h_{fp} d_p}{k_f} = 2 + 1.1 Pr^{\frac{1}{3}} Re_p^{0.6};\ Pr = \frac{k_f c_{p,f}}{\mu_f};\ Re_p = \frac{\rho_f d_p \varepsilon u_f}{\mu_f} \tag{19}$$

For calculating the porosity of the bed, Eq. (20) is used. [25]

$$\varepsilon = 0.375 + 0.17 \frac{d_p}{D} + 0.39 \left(\frac{d_p}{D}\right)^2 \tag{20}$$

The heat loss to the ambient is calculated based on the overall heat transfer coefficient from the inner to the outer wall, see Eq. (21). The inner convection heat transfer coefficient is defined according to Beek [26], see Eq. (22).

$$\frac{1}{U_w} = \frac{1}{h_i} + \frac{D}{2} \sum_{j=1}^{m} \frac{1}{k_j} ln \left(\frac{d_{j+1}}{d_j}\right) \tag{21}$$

$$h_i = \frac{k_f}{d_p} \left[\left(0.203 Pr^{\frac{1}{3}} Re_p^{\frac{1}{3}}\right) + \left(0.220 Pr^{0.4} Re_p^{0.8}\right) \right] \tag{22}$$

where h_i is the inner convection heat transfer coefficient, Re is Reynolds number, and Pr is the Prandtl number.

The governing equations are solved by the MATLAB software [27] using finite difference method and the implicit method. The first-order upwind scheme is used to discretize the temporal and advective term, while the second-order central differencing is used to discretize the diffusion term. The overall calculation method is illustrated in Figure 3.

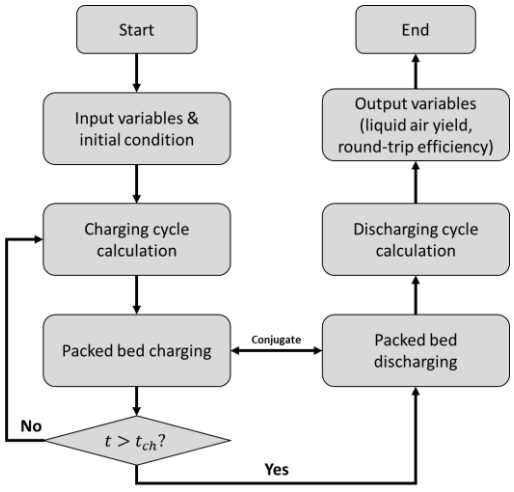

Figure. 3. *Overall calculation method of the LAES system.*

Table 2 represents the thermophysical properties of the quartz rocks [3] besides, the cryogenic PCM which is an alcohol-based fluid [11]. The thermophysical properties of silicon dioxide (SiO_2) are calculated based on correlations as a function of the particles' temperature proposed by Wang et al. [9] and Sciacovelli et al. [13].

Table. 2. *Thermophysical properties of particles [11,25].*

Properties	PCM	$Quartz$
Density, ρ	789.3 kg/m^3	2630 kg/m^3
Specific heat, C_p	1850 $J/kg\ K$, Solid	710 $J/kg\ K$
	1900 $J/kg\ K$, Liquid	
Thermal conductivity, k	0.22 $W/m\ K$, Solid	1.83 $W/m\ K$
	0.18 $W/m\ K$, Liquid	
Latent heat, L_H	86000 J/kg	-
Melting Point, T_m	155.15 K T_{m1}	-
	158.15 K, T_{m2}	

3. Results and discussion

In this section, first, the validation of the packed bed model is presented. Then the optimum value for discharging pressure is found based on a sensitivity analysis. Afterwards, the different particle materials are compared in terms of LAES round-trip efficiency, liquid air yield, and gas turbine power.

3.1 Model validation

The developed model for the packed bed is validated by comparing the results with experimental data from a study by Li et al. [28] who analysed a packed bed system with microencapsulation of molten salt as phase change material. The packed bed in their study had a height of 0.26 m and a diameter of 0.26 m. The particle diameter was 0.034 m. The authors considered both the axial and radial temperature distribution along the bed's tank by applying thermocouples at various locations of the tank. When validating results of the 1D model developed in this work, the mean value of the radial temperature distribution at each axial location of the experimental data is considered. Figure 4 presents a comparison of the model results with the experimental data showing PCM particle temperature profiles over time for different axial locations. It is found that the maximum mean absolute percentage error is smaller than 2 %, suggesting that the current model provides reasonable results.

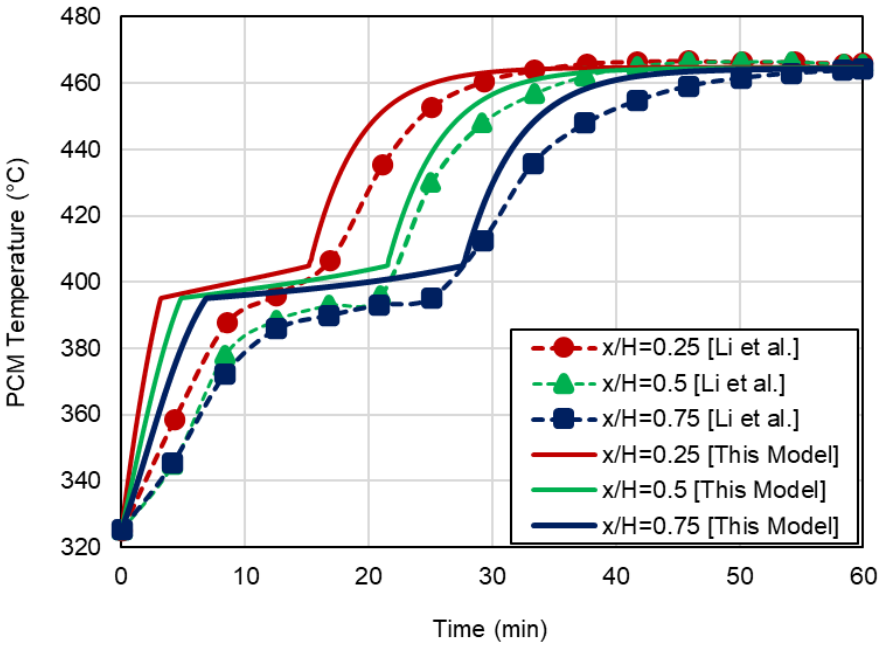

Figure. 4. *Validation of packed bed model.*

The validation of the LAES thermodynamic model is done by comparing the current model results with experimental results presented by Sciacovelli et al. [13], see Table 3. The experimental setup of the Sciacovelli et al. [13] research study only contains the LAES discharging cycle. The mass flow rate of air is

1.8 kg/s in that setup. The results presented in Table 3 indicate that the thermodynamic models developed in the current work provide reasonable results.

Table. 3. *The results of current model compared to the results from [13].*

Parameter	Results of the current model	Results of Ref. [13]	Deviation
Turbines' power	277.77 kW	277.85 kW	0.38 %
Cryo-pump's power	29.79 kW	30.01 kW	0.73 %

3.2 Optimal discharging pressure

Two important parameters of LAES systems that have a significant influence on their overall performance are the charging and discharging pressures. In this paper the charging pressure was defined and kept constant, while it is required to evaluate the optimum value of the discharging pressure. Figure 5 presents the LAES round-trip efficiency, cryo-pump power consumption, turbine power output, and net power output of the discharging cycle versus the discharging pressure varying from 10 MPa to 25 MPa. The results indicate that the round-trip efficiency increases with the increase of discharging pressure. However, the more dominant effect of the increase in discharging pressure is on the cryo-pump power consumption, which is increasing sharply with increasing discharging pressure. According to Figure 5, the additional gain in round-trip efficiency is small for discharging pressures exceeding 18 MPa. Thus, the discharging pressure is set to 20 MPa (purple band in Figure 5), resulting in a round-trip efficiency of 41 %, cryo-pump power consumption of 2.6 MW, turbine power output 42 MW, and hence a net power output of 39.4 MW.

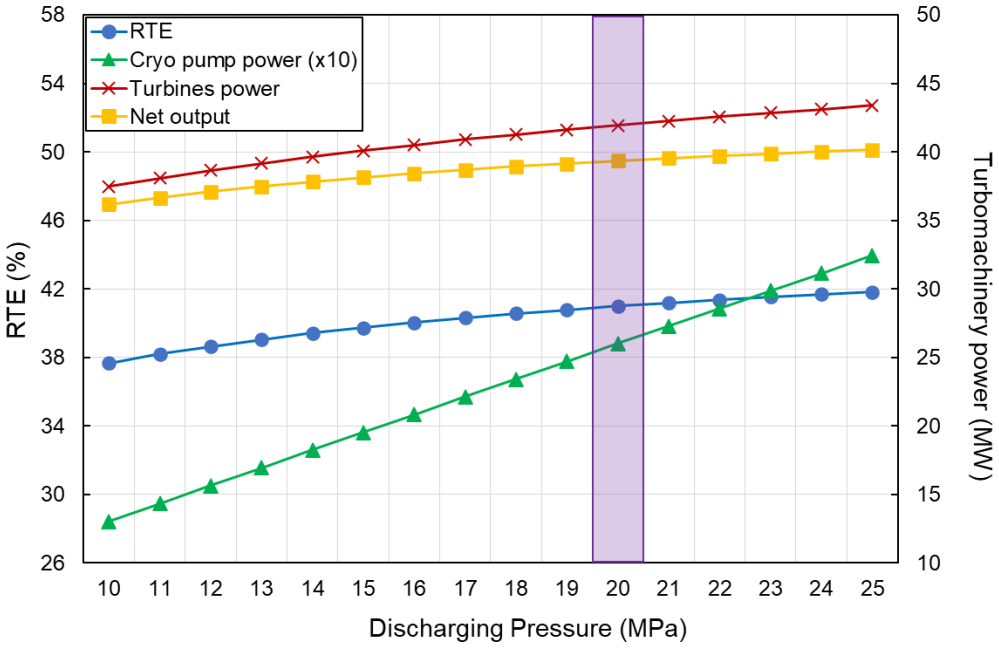

Figure. 5. *LAES round-trip efficiency, cryo-pump power consumption, turbine power output, and net power output of the discharging cycle versus the discharging pressure.*

3.3 Performance of LAES system with different particles in the packed bed

Figure 6 presents a comparison of the LAES round-trip efficiency, mean liquid air yield, and turbine power output for packed bed systems with the three different particles for the cold energy storage. The results suggest that the SiO2 particle results in the poorest performance, while the PCM and quartz particles attain very similar performances.

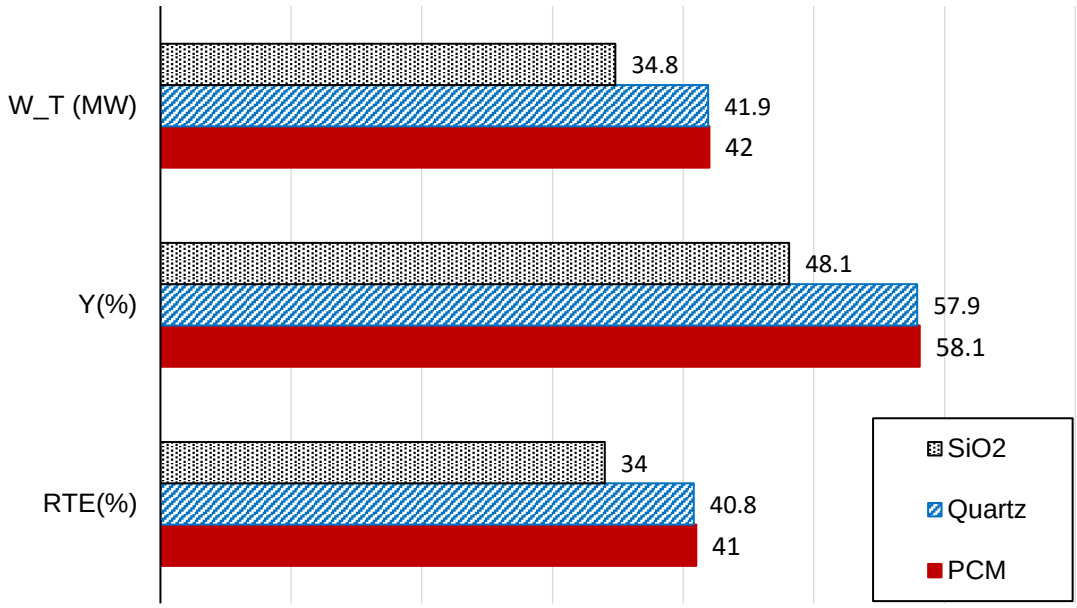

Figure. 6. *Round-trip efficiency (RTE), mean liquid air yield (Y), and output power of the turbines ($\dot{W}_T$) for the three different particle types.*

In order to understand the effects of the particle materials, Figure 7 presents the heat transfer fluid temperature at the outlet of the packed bed (point C1 in Figure 1) versus time for the three different particle materials. The outlet temperature of the air starts to increase after 66 minutes, 128 minutes and 161 minutes for the SiO2, PCM and quartz, respectively. The temperature of point C1 directly affects on the temperature of point A8, the parameter, which have a significant influence on the liquid air yield, the round-trip efficiency and the output power of the turbines. A lower temperature in point A8 results in a higher liquid air yield. The poor performance of SiO2 particles is because of the rapid increase in temperature of C1 (Figure 7), due to unfavourable thermophysical properties of SiO2 in terms of specific heat capacity and density in comparison with PCM and quartz. In contrast, the increase of air temperature over time for the cases of PCM and quartz is controlled in a better way and as a result, these two systems present better performance due to a lower temperature at the inlet of cold box. The phase change phenomenon of PCM is noticeable in the temperature range around the PCM melting point (155 K to 158 K), where the air temperature remains constant for the rest of the charging time. It can be observed that the outlet temperature (C1) does not exceed the melting point of PCM since there are still some particles in the solid state. The reason why the quartz particle achieves similar performance as that of the PCM, although it is not a phase change material, is that quartz particle keeps the air temperature equal to the packed bed's initial charging temperature for a longer time duration than does the PCM. This is because the density of quartz particles is more than 3 times higher than that of the PCM considered for the analysis. As the volume of the packed bed and the porosity are the same for all 3 particle materials, the higher particle density results in a higher particle mass. Therefore, the storage mass of the quartz system is more than 3 times than that of the PCM for the same volume of the packed bed system.

The behaviour of liquid yield over time for the three particle materials is presented in Figure 8. Similar to the temperature in point C1, the liquid yield is constant while the PCM changes phase, reaching a steady state of 0.467 after 354 min. The maximum value of the liquid yield (slightly above 0.7) is attained for the longest duration for the quartz particles because the temperature in point C1 is kept at the minimum value for the longest duration for this material. The liquid yield starts to decrease from the maximum value after 199 min, 160 min and 87 min for the quartz, PCM and SiO2, respectively.

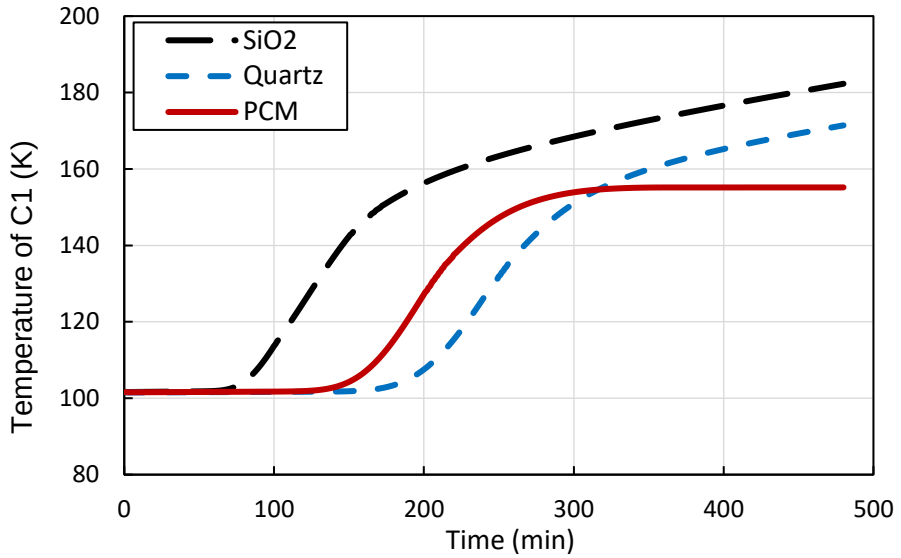

Figure. 7. *Air temperature at the outlet of packed bed versus charging time for the three different particles, SiO2, quartz and PCM.*

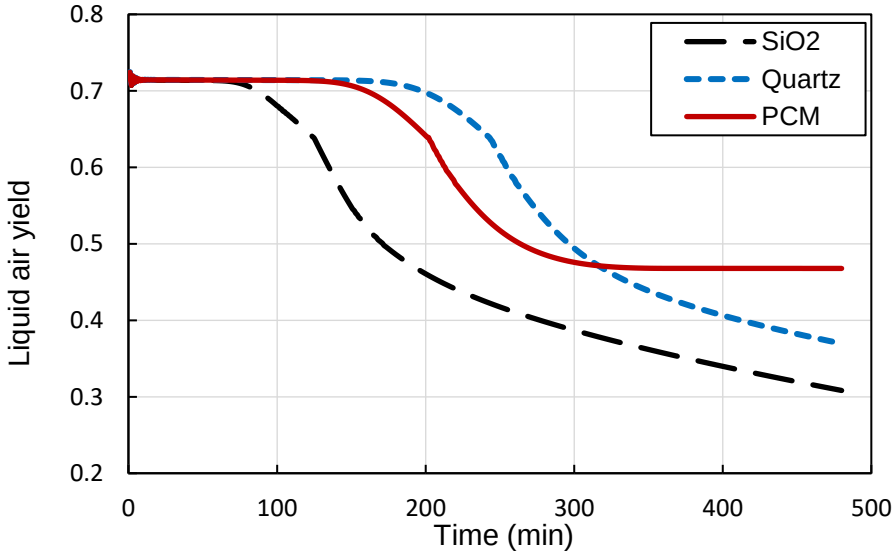

Figure. 8. *LAES liquid yield versus time for the three types of particles.*

4. Conclusions

In this paper a comparative analysis of sensible heat and latent heat packed bed cold energy storages for LAES systems was presented. The investigated particles are quartz and silicon dioxide representing sensible heat storage materials and an alcohol-based fluid representing a latent heat phase change material. A thermodynamic model of the LAES system integrated with a 1-dimensional transient numerical model of the packed bed system was developed. The particles were compared in terms of the LAES round-trip efficiency, mean liquid yield, and output power of the turbines. The results suggest that the optimum value for discharging pressure of the system is 20 MPa. Among the analysed particle materials, the PCM and quartz achieve the highest round-trip efficiency for the LAES system, 41 % and 40.8 %, respectively. The round-trip efficiency of the silicon dioxide is lower, 34 %, due to unfavourable thermophysical properties. The reason why the quartz particle achieves similar performance as that of the PCM, although it is not a phase change material, is that quartz particle keeps the air temperature at the cold storage outlet equal to the packed bed's initial charging temperature for a longer time duration than does the PCM. This is because the density of quartz particles is more than 3 times higher than that of the PCM considered for the analysis, resulting in a greater mass of the cold storage based on quartz. In general, the choice between PCM particles and quartz particles for a LAES cold storage system depends on factors such as the required energy density, the desired charging and discharging rates, the available space and weight limits, and the cost of the materials. These aspects will be investigated in future work.

Acknowledgment

The research presented in this paper was partly developed within the project “Sustainable large-scale energy storage in Egypt” (Project no. 21-M13-DTU), funded by the Ministry of Foreign Affairs of Denmark and administrated by Danida Fellowship Centre. In addition, the research was partly funded by a Korea Agency for Infrastructure Technology Advancement (KAIA) grant provided by the Ministry of Land, Infrastructure and Transport (Grant RS-2022-00143652). The financial support is gratefully acknowledged.

Nomenclature

C_p	Specific heat capacity, $J/kg.K$	$\dot{Q}$	Heat transfer rate, W
CRP	Cryogenic pump	r	Radial location inside each particle, m
CTB	Cryogenic turbine	R	Particles radius, m
D	Packed bed diameter, m	RTE	Round-trip efficiency
d_p	Particles diameter, m	t	Time, s
H	Packed bed height, m	T	Temperature, K
h	Specific enthalpy, J/kg	u_f	Velocity of air inside packed bed, m/s
h_{fp}	Convective heat transfer coefficient between air and particles, $W/m^2.K$	$\dot{W}$	Turbomachinery power, W
h_w	Convective heat transfer coefficient between packed bed and ambient, $W/m^2.K$	y	Liquid air yield
k	Thermal conductivity, $W/m.K$	Y	Mean liquid air yield
$\dot{m}$	Mass flow rate, kg/s	z	Axial location of packed bed tank, m
P	Pressure, Pa		

Greek symbols

ε	Porosity of packed bed	μ	Dynamic viscosity, $Pa.s$
η	Isentropic efficiency of turbomachinery	ρ	Density, kg/m^3

Subscripts and superscripts

amb	Ambient	p	Particle
C	Compressor	s	Solid particles inside packed bed
f	Fluid	T	Turbine

Reference

[1] Lin B, Wu W, Bai M, Xie C. Liquid air energy storage: Price arbitrage operations and sizing optimization in the GB real-time electricity market. Energy Econ 2019;78:647–55. https://doi.org/10.1016/J.ENECO.2018.11.035.

[2] Tafone A, Romagnoli A, Li Y, Borri E, Comodi G. Techno-economic Analysis of a Liquid Air Energy Storage (LAES) for Cooling Application in Hot Climates. Energy Procedia 2017;105:4450–7. https://doi.org/10.1016/J.EGYPRO.2017.03.944.

[3] Morgan R, Nelmes S, Gibson E, Brett G. An analysis of a large-scale liquid air energy storage system. Proceedings of Institution of Civil Engineers: Energy 2015;168:135–44. https://doi.org/10.1680/ener.14.00038.

[4] She X, Peng X, Nie B, Leng G, Zhang X, Weng L, et al. Enhancement of round trip efficiency of liquid air energy storage through effective utilization of heat of compression. Appl Energy 2017;206:1632–42. https://doi.org/10.1016/J.APENERGY.2017.09.102.

[5] Antonelli M, Barsali S, Desideri U, Giglioli R, Paganucci F, Pasini G. Liquid air energy storage: Potential and challenges of hybrid power plants. Appl Energy 2017;194:522–9. https://doi.org/10.1016/J.APENERGY.2016.11.091.

[6] Peng X, She X, Cong L, Zhang T, Li C, Li Y, et al. Thermodynamic study on the effect of cold and heat recovery on performance of liquid air energy storage. Appl Energy 2018;221:86–99. https://doi.org/10.1016/J.APENERGY.2018.03.151.

[7] Xu C, Li X, Wang Z, He Y, Bai F. Effects of solid particle properties on the thermal performance of a packed-bed molten-salt thermocline thermal storage system. Appl Therm Eng 2013;57:69–80. https://doi.org/10.1016/J.APPLTHERMALENG.2013.03.052.

[8] Borri E, Sze JY, Tafone A, Romagnoli A, Li Y, Comodi G. Experimental and numerical characterization of sub-zero phase change materials for cold thermal energy storage. Appl Energy 2020;275:115131. https://doi.org/10.1016/J.APENERGY.2020.115131.

[9] Wang C, Bian Y, You Z, Luo Y, Zhang X, Peng H, et al. Dynamic analysis of a novel standalone liquid air energy storage system for industrial applications. Energy Convers Manag 2021;245:114537. https://doi.org/10.1016/J.ENCONMAN.2021.114537.

[10] Ryu JY, Alford A, Lewis G, Ding Y, Li Y, Ahmad A, et al. A novel liquid air energy storage system using a combination of sensible and latent heat storage. Appl Therm Eng 2022;203. https://doi.org/10.1016/j.applthermaleng.2021.117890.

[11] Tafone A, Borri E, Cabeza LF, Romagnoli A. Innovative cryogenic Phase Change Material (PCM) based cold thermal energy storage for Liquid Air Energy Storage (LAES) – Numerical dynamic modelling and experimental study of a packed bed unit. Appl Energy 2021;301. https://doi.org/10.1016/j.apenergy.2021.117417.

[12] Bashiri Mousavi S, Ahmadi P, Hanafizadeh P, Khanmohammadi S. Dynamic simulation and techno-economic analysis of liquid air energy storage with cascade phase change materials as a cold storage system. J Energy Storage 2022;50:104179. https://doi.org/10.1016/J.EST.2022.104179.

[13] Sciacovelli A, Vecchi A, Ding Y. Liquid air energy storage (LAES) with packed bed cold thermal storage – From component to system level performance through dynamic modelling. Appl Energy 2017;190:84–98. https://doi.org/10.1016/j.apenergy.2016.12.118.

[14] Guo L, Ji W, Gao Z, Fan X, Wang J. Dynamic characteristics analysis of the cold energy transfer in the liquid air energy storage system based on different modes of packed bed. J Energy Storage 2021;40. https://doi.org/10.1016/j.est.2021.102712.

[15] Tafone A, Romagnoli A, Borri E, Comodi G. New parametric performance maps for a novel sizing and selection methodology of a Liquid Air Energy Storage system. Appl Energy 2019;250:1641–56. https://doi.org/10.1016/J.APENERGY.2019.04.171.

[16] Wang C, Cui Q, Dai Z, Zhang X, Xue L, You Z, et al. Performance analysis of liquid air energy storage with enhanced cold storage density for combined heating and power generation. J Energy Storage 2022;46. https://doi.org/10.1016/j.est.2021.103836.

[17] Hüttermann L, Span R. Investigation of storage materials for packed bed cold storages in liquid air energy storage (LAES) systems. Energy Procedia 2017;143:693–8. https://doi.org/10.1016/J.EGYPRO.2017.12.748.

[18] Peng H, Shan X, Yang Y, Ling X. A study on performance of a liquid air energy storage system with packed bed units. Appl Energy 2018;211:126–35. https://doi.org/10.1016/J.APENERGY.2017.11.045.

[19] Cascetta M, Cau G, Puddu P, Serra F. Numerical investigation of a packed bed thermal energy storage system with different heat transfer fluids. Energy Procedia, vol. 45, Elsevier Ltd; 2014, p. 598–607. https://doi.org/10.1016/j.egypro.2014.01.064.

[20] Ortega-Fernández I, Loroño I, Faik A, Uriz I, Rodríguez-Aseguinolaza J, D'Aguanno B. Parametric analysis of a packed bed thermal energy storage system. AIP Conf Proc, vol. 1850, American Institute of Physics Inc.; 2017. https://doi.org/10.1063/1.4984442.

[21] Knobloch K, Muhammad Y, Costa MS, Moscoso FM, Bahl C, Alm O, et al. A partially underground rock bed thermal energy storage with a novel air flow configuration. Appl Energy 2022;315:118931. https://doi.org/10.1016/J.APENERGY.2022.118931.

[22] Cohen Y, Metzner AB. Wall effects in laminar flow of fluids through packed beds. AIChE Journal 1981;27:705–15. https://doi.org/10.1002/aic.690270502.

[23] Ahmed N, Elfeky KE, Qaisrani MA, Wang QW. Numerical characterization of thermocline behaviour of combined sensible-latent heat storage tank using brick manganese rod structure impregnated with PCM capsules. Solar Energy 2019;180:243–56. https://doi.org/10.1016/j.solener.2019.01.001.

[24] Ewl, Ihb, MH, MML. REFPROP Documentation. 2018.

[25] Wakao N, Kaguei S, Funazkri T. Effect of fluid dispersion coefficients on particle-to-fluid heat transfer coefficients in packed beds: Correlation of nusselt numbers. Chem Eng Sci 1979;34:325–36. https://doi.org/10.1016/0009-2509(79)85064-2.

[26] Beek J. DESIGN OF PACKED CATALYTIC REACTORS. n.d.

[27] Mathworks®. MATLAB® 2022a.

[28] Li MJ, Jin B, Ma Z, Yuan F. Experimental and numerical study on the performance of a new high-temperature packed-bed thermal energy storage system with macroencapsulation of molten salt phase change material. Appl Energy 2018;221:1–15. https://doi.org/10.1016/j.apenergy.2018.03.156.